UNIVERSITY
OF TRENTO

DIPARTIMENTO DI INGEGNERIA E SCIENZA DELL'INFORMAZIONE

38123 Povo – Trento (Italy), Via Sommarive 14
http://www.disi.unitn.it

AN EFFECTIVE EXCITATION MATCHING METHOD FOR THE SYNTHESIS OF OPTIMAL COMPROMISES BETWEEN SUM AND DIFFERENCE PATTERNS IN PLANAR ARRAYS

P. Rocca, L. Manica, and A. Massa

January 2008

Technical Report # DISI-11-053

An Effective Excitation Matching Method for the Synthesis of Optimal Compromises between Sum and Difference Patterns in Planar Arrays

P. Rocca, L. Manica, and A. Massa, *EM Academy Fellow*

ELEDIA Research Group

Department of Information and Communication Technology,

University of Trento, Via Sommarive 14, 38050 Trento - Italy

Tel. +39 0461 882057, Fax +39 0461 882093

E-mail: *andrea.massa@ing.unitn.it*,

{*paolo.rocca, luca.manica*}*@dit.unitn.it*

Web: *http://www.eledia.ing.unitn.it*

An Effective Excitation Matching Method for the Synthesis of Optimal Compromises between Sum and Difference Patterns in Planar Arrays

P. Rocca, L. Manica, and A. Massa

Abstract

In this paper, the extension of the *Contiguous Partition Method* (CPM) from linear to planar arrays is described and assessed. By exploiting some properties of the solution space, the generation of compromise sum-difference patterns is obtained through an optimal excitation matching procedure based on a combinatorial method. The searching of the solution is carried out thanks to an efficient path-searching algorithm aimed at exploring the solution space represented in terms of a graph. A set of representative results are reported for the assessment as well as for comparison purposes.

Key words: Planar Arrays, Compromise patterns, Sum and difference modes, Direct acyclic graph.

1 Introduction

In antenna design, the optimal synthesis of sum and difference patterns is a classical problem. In such a framework, the synthesis of array antennas able to generate both a sum pattern and a difference one has received some attention because of their applications in radar searching and tracking [1][2]. Since exact methods of synthesizing independently optimum sum and difference arrays exist for both linear [3]-[6] and planar architectures [7][8], whether the complexity and cost of the arising feed networks are affordable, then the above methods can be directly used. However, since the implementation of two (or three) totally independent signal feeds is generally expensive and complex, a number of alternative solutions have been proposed to generate the two or three required patterns via shared feed networks at the cost of a reduction in the quality of one or more patterns [2][9].

In order to avoid the need of a completely different feeding (receiving) network for each operation mode, several researches [10]-[15] proposed to partition the original array in sub-arrays. In such a scheme, the feeding network is usually devoted to the optimization of the sum channel, so that the excitations of the arrays elements for such a mode correspond to the optimal one (e.g., Dolph-Chebyshev [3]). Then, the difference mode is obtained thanks to a suitable choice of the weight of each sub-array. Consequently, a large part of the whole architecture is common to both modes with a non negligible saving of costs. On the other hand, a compromise difference pattern is obtained. The degree of optimality of the compromise solution is related to the number of sub-arrays, which establishes a trade-off between costs and performances. As a matter of fact, a large number of sub-arrays allows better performances, but also implies higher costs. Otherwise, few sub-arrays may imply unacceptable difference patterns. For a fixed number of sub-arrays, once the excitations of the sum pattern have been fixed, the problem is concerned with the grouping of the array elements into sub-arrays and the computation of their weights to determine the best compromise difference pattern.

As far as the number of unknowns is concerned, it grows proportionally to the dimension of the array and, usually, it turns out to be very large when real applications of planar arrays are considered. Consequently, a standard use of global optimization techniques is not convenient since a suboptimal solution is generally obtained in the limited time one has at his disposal. As a matter of fact, the arising computational burden raises very rapidly with the dimension of

the solution space. Although this circumstance is quite underestimated in antenna design since synthesis problems may have many different satisfactory suboptimal solutions, nevertheless they can be significantly worse than the global ones.

In order to overcome such drawbacks, in Ares et *al.* [11] the antenna aperture has been divided into four quadrants and the monopulse function has been obtained by combining the outputs in a monopulse comparator. The sum pattern and the difference one have been generated with all quadrants added in phase and with pairs of quadrants added in phase reversal, respectively. Moreover, in order to reduce the number of unknowns, each antenna quadrant has been *a-priori* divided into sub-arrays (i.e., the sectors) and only the sub-array weights have been calculated by minimizing a suitable cost function again according to a Simulated Annealing (SA) algorithm. In an alternative fashion, D'Urso et *al.* [14] formulated the problem in such a way that global optimization tools have to deal with a reduced number of unknowns. By exploiting the convexity of the cost functional to be minimized with respect to a part of the unknowns (i.e., the sub-array gains), an hybrid two-step optimization strategy has been applied instead of simultaneously optimizing (in the same way) both the involved variables. As a matter of fact, once the clustering into sub-arrays has been determined by using a SA technique, the problem at hand gives rise to a Convex Programming (CP) problem with a single minimum that can be retrieved with a local optimization technique. Unfortunately, although unlike [11] no *a-priori* informations are necessary, the evaluation of the auxiliary CP objective function is usually more cumbersome than the original cost function. Such an event could result in an excessively large computational burden that would prevent the retrieval of the global optimum in the available amount of time or to efficiently deal with large planar arrays.

In [15], a computationally-effective method for the optimal compromise among sum and difference patterns has been proposed to deal with linear arrays. The optimization problem has been recast as a combinatorial one, thus significantly reducing the dimension of the solution space and allowing a fast synthesis process. Because of its computational efficiency, such a technique seems to be a good candidate to deal also with two-dimensional ($2D$) arrays in order to overcome the computational drawbacks of stochastic optimization methodologies. Towards this end, a suitable implementation (not a simple extension) is mandatory to keep also in the planar case the best features of the linear approach both in term of reliability and computational

efficiency. As a matter of fact, unlike the linear case, the planar structure requires two difference patterns (i.e., the difference $E-mode$ and the $H-mode$). Moreover, the dimensionality of the problem at hand significantly grows with respect to the linear situation, thus enhancing the computational problems in applying global optimization methodologies and thus preventing their use also in hybrid modalities.

Therefore this paper is aimed at describing and assessing the planar extension of the CPM (in the following $PCPM$) according to the following outline. The mathematical formulation is presented in Sect. 2 pointing out the main differences compared to the linear array case. Section 3 is devoted to the numerical assessment. Both a consistency check, carried out through an asymptotic study, and a comparative analysis (unfortunately, just only a test case is available in the recent literature) are considered. Finally, some comments are drawn in the concluding section (Sect. 4).

2 Mathematical Formulation

Let us consider a planar array lying on the $xy-plane$ whose array factor is given by

$$AF(\theta,\phi)=\sum_{r=-R}^{R}\sum_{s=-S(r)}^{S(r)}\xi_{rs}e^{j(k_x x_r+k_y y_s)},\quad n,m\neq 0 \tag{1}$$

where $x_r=\left[r-\frac{sgn(r)}{2}\right]\times d_x$ and $y_s=\left[s-\frac{sgn(s)}{2}\right]\times d_y$, d_x and d_y being the inter-element distance along the x and y direction, respectively. Moreover, $k_x=\frac{2\pi}{\lambda}sin\theta cos\phi$ and $k_y=\frac{2\pi}{\lambda}sin\theta sin\phi$. Concerning independently optimum sum and difference patterns, they are generated by using three independent feeding networks and setting the excitation vector $\underline{\xi}=\{\xi_{rs};\ r=\pm1,...,\pm R;\ s=\pm1,...,\pm S(r)\}$ to $\underline{\zeta}=\left\{\zeta_{rs}=\zeta_{(-r)s}=\zeta_{r(-s)}=\zeta_{(-r)(-s)};\ r=1,...,R;\ s=1,...,S(r)\right\}$ and to $\underline{\varsigma}^{\triangle}=\left\{\varsigma^{\triangle}_{rs}=\varsigma^{\triangle}_{(-r)s}=-\varsigma^{\triangle}_{r(-s)}=-\varsigma^{\triangle}_{(-r)(-s)};\ r=1,...,R;\ s=1,...,S(r)\right\}$, $\triangle=E,\ H$, respectively. Otherwise, when sub-arraying strategies are considered [**?**], the sum beam is generated in an optimal fashion by fixing $\underline{\xi}=\underline{\zeta}$, while the compromise $\triangle-$modes are obtained through a grouping operation described by the aggregation vectors $\underline{c}^{\triangle}$

$$\underline{c}^{\triangle}=\left\{c^{\triangle}_{rs};\ r=1,...,R;\ s=1,...,S(r)\right\} \tag{2}$$

where $c_{rs}^{\triangle} \in [1, Q]$ is the sub-array index of the element located at the r-th row and s-th column within the array architecture. Accordingly, the compromise difference excitations are given by

$$\underline{\gamma}^{\triangle} = \left\{ \gamma_{rs}^{\triangle} = \zeta_{rs} O\left(c_{rs}^{\triangle},\, q\right) g_q^{\triangle};\; r = 1, ..., R;\; s = 1, ..., S(r);\; q = 1, ..., Q \right\} \tag{3}$$

where $g_q^{\triangle}$ is the gain coefficient of the q-th sub-array and $O\left(c_{rs}^{\triangle},\, q\right) = 1$ if $c_{rs}^{\triangle} = q$ and $O\left(c_{rs}^{\triangle},\, q\right) = 0$, otherwise. Summarizing, the problem of defining the best compromise between sum and difference patterns is recast as the definition of the configuration $\underline{c}_{opt}^{\triangle}$ and the corresponding set of weights $\underline{g}_{opt}^{\triangle}$ so that $\underline{\gamma}_{opt}^{\triangle}$ is as close as much as possible to $\underline{\varsigma}^{\triangle}$.
Towards this end, the CPM is applied. Similarly to the linear array case, the following cost function is defined

$$\Psi\left(\underline{c}^{\triangle}\right) = \frac{\sum_{q=1}^{Q} \sum_{r=1}^{R} \sum_{s=1}^{S(r)} \zeta_{rs}^2 \left| \left[\alpha_{rs}^{\triangle} - w_{rsq}\left(\underline{c}^{\triangle}\right) \right] \right|^2}{N} \tag{4}$$

where N is the number of elements lying on the aperture [i.e., $N = \sum_{r=1}^{R} S(r)$]. Moreover, $\alpha_{rs}^{\triangle} = \frac{\varsigma_{rs}^{\triangle}}{\zeta_{rs}}$ and $w_{rsq}^{\triangle} = w_{rsq}\left(\underline{c}^{\triangle}\right)$ is given by

$$w_{rsq}^{\triangle} = \frac{\sum_{r=1}^{R} \sum_{s=1}^{S(r)} \zeta_{rs}^2 O\left(c_{rs}^{\triangle},\, q\right) \alpha_{rs}^{\triangle}}{\sum_{r=1}^{R} \sum_{s=1}^{S(r)} \zeta_{rs}^2 O\left(c_{rs}^{\triangle},\, q\right)}, \quad r = 1, ..., R;\;\; s = 1, ..., S(r);\;\; q = 1, ..., Q. \tag{5}$$

As regards to the sub-array weights, they are computed once the aggregation vector $\underline{c}^{\triangle}$ has been identified by simply using the following relationship

$$g_q^{\triangle} = O\left(c_{rs}^{\triangle},\, q\right) w_{rsq}^{\triangle} \qquad r = 1, ..., R;\;\; s = 1, ..., S(r);\;\; q = 1, ..., Q. \tag{6}$$

In order to determine the unknown clustering that minimizes (4), the indication given in [16] has been exploited. More in detail, it has been proved that a *contiguous partition*[(1)] of the array elements is the optimal compromise solution. Accordingly, the set of contiguous partitions (i.e., the set of admissible solutions) is defined by iteratively partitioning in Q sub-sets the list

[(1)] A grouping of array elements is a contiguous partition if the generic (r_2, s_2)-th array element belongs to the q-th sub-array only when two elements, namely the (r_1, s_1)-th element and the (r_3, s_3)-th one, belong to the same sub-array and the condition $\alpha_{r_1 s_1}^{\triangle} < \alpha_{r_2 s_2}^{\triangle} < \alpha_{r_3 s_3}^{\triangle}$ holds true.

$V = \{v_n;\, n = 1, ..., N\}$ (n being the list index) of the array elements ordered according to the corresponding $\alpha_{rs}^{\triangle}$ values such that $v_n \leq v_{n+1}$ ($n = 1, ..., N-1$), $v_1 = min_{rs}\left\{\alpha_{rs}^{\triangle}\right\}$, $v_N = max_{rs}\left\{\alpha_{rs}^{\triangle}\right\}$.

Although the dimension of the $PCPM$ solution space, $\Im^{PCPM}$, is significantly reduced compared to that of full global optimizers [$D^{(PCPM)} = \begin{pmatrix} N-1 \\ Q-1 \end{pmatrix}$ vs. $D^{(GA)} = Q\left(Q^{N-1}+1\right)$] or hybrid global-local optimization techniques [$D^{(Hybrid)} = Q^N$], non-negligible computational problems still remain since the large amount of computational resources needed to sample $\Im^{PCPM}$ especially when N enlarges as it happens in realistic planar architecture. Therefore, it is mandatory to devise an effective sampling procedure able to guarantee a good trade-off between computational costs and optimality of the synthesized compromise solution. Towards this end, the set of admissible solutions has been coded into a *Direct Acyclic Graph* (DAG). The DAG is composed by Q rows and N columns. The q-th row is related to the q-th sub-array ($q = 1, ..., Q$), whereas the n-th column ($n = 1, ..., N$) maps the v_n-th element of the ordered list V. An admissible compromise solution is coded into a path, denoted by ψ, in the DAG. Each path ψ is described by a set of N vertexes, $\{t_n;\, n = 1, ..., N\}$ and through $N-1$ relations/links $\{e_n;\, n = 1, ..., N-1\}$ among the vertexes belonging to the path. With reference to Fig. 1, each vertex t_n is indicated by a circle and each link e_n with an arrow from a vertex t_n to another one t_{n+1} on the same row [i.e., $arg\left(t_n\right) = arg\left(t_{n+1}\right) = r_n$, being r_n the row of the n-th vertex, $r_n \in [1,\, Q]$] or down to an adjacent row [i.e., $arg\left(t_{n-1}\right) = r_n$ and $arg\left(t_n\right) = r_n + 1$].

In order to identify the optimal compromise (or, in an equivalent fashion, the optimal path ψ_{opt} in the DAG), let us reformulate the concept of "*border elements*" of the linear case to the planar representation in terms of DAG. Moreover, let us consider that analogously to the linear case, only the "*border elements*" of ψ (i.e., those vertexes t_n, $n = 2, ..., N-1$ having at most one of the adjacent vertexes, t_{n-1} or t_{n+1}, that belongs to a different row of the DAG) are candidate to change their sub-array membership without generating non-admissible aggregations. Accordingly, in order to determine the optimal sub-array configuration $\underline{c}_{opt}^{\triangle}$ that minimizes $\Psi\left(\underline{c}^{\triangle}\right)$ (4), a sequence of trial paths $\psi^{(k)} = \left\{\left(t_n^{(k)}, e_m^{(k)}\right);\, n = 1, ..., N;\, m = 1, ..., N-1\right\}$ (k being the iteration/trial index) is generated. Starting from an initial path $\psi^{(k)}$ ($k = 0$) defined by setting $arg\left(t_1^{(0)}\right) = 1$ and $arg\left(t_N^{(0)}\right) = Q$ and randomly choosing the other vertexes such as $arg\left(t_{n-1}^{(0)}\right) \leq arg\left(t_n^{(0)}\right) \leq arg\left(t_{n+1}^{(0)}\right)$, the path $\psi^{(k)}$ is iteratively updated ($\psi^{(k)} \leftarrow \psi^{(k+1)}$,

$\underline{c}^{\triangle(k)} \leftarrow \underline{c}^{\triangle(k+1)}$) just modifying the memberships of the border elements of the DAG. More in detail, the "*border*" vertexes are updated as follows

$$arg\left(t_n^{(k+1)}\right) = \begin{cases} r_n^{(k)} + 1 & if \quad r_{n-1}^{(k)} = r_n^{(k)} \\ r_n^{(k)} - 1 & if \quad r_{n+1}^{(k)} = r_n^{(k)} \end{cases}, \tag{7}$$

while the links $e_{n-1}^{(k)} \triangleq link\left[arg\left(t_{n-1}^{(k)}\right), arg\left(t_n^{(k)}\right)\right]$ and $e_n^{(k)} \triangleq link\left[arg\left(t_n^{(k)}\right), arg\left(t_{n+1}^{(k)}\right)\right]$ connected to the "border" vertex $t_n^{(k)}$ are modified through the relationships

$$e_{n-1}^{(k+1)} = \begin{cases} link\left[r_n^{(k)}, r_n^{(k)} + 1\right] & if \quad r_{n-1}^{(k)} = r_n^{(k)} \\ link\left[r_n^{(k)} - 1, r_n^{(k)} - 1\right] & if \quad r_{n+1}^{(k)} = r_n^{(k)} \end{cases} \tag{8}$$

and

$$e_n^{(k+1)} = \begin{cases} link\left[r_n^{(k)} + 1, r_n^{(k)} + 1\right] & if \quad r_{n-1}^{(k)} = r_n^{(k)} \\ link\left[r_n^{(k)} - 1, r_n^{(k)}\right] & if \quad r_{n+1}^{(k)} = r_n^{(k)} \end{cases}. \tag{9}$$

The iterative process stops when a maximum number of iterations K_{max} ($k > K_{max}$) or the following stationary condition holds true:

$$\frac{\left|K_w \Psi^{(k-1)} - \sum_{h=1}^{K_w} \Psi^{(h)}\right|}{\Psi^{(k)}} \leq \eta \tag{10}$$

where $\Psi^{(k)} = \Psi\left(\underline{c}^{\triangle(k)}\right)$, K_w and η being a fixed number of iterations and a fixed numerical threshold, respectively. At the end of the iterative sampling of the DAG, the path ψ^{opt} is found and the corresponding aggregation vector, $\underline{c}_{opt}^{\triangle}$, is assumed as the optimal compromise solution.

3 Numerical Results

This section is aimed at assessing the effectiveness of the $PCPM$ through a set of representative results from several numerical simulations. The remaining of this section is organized as follows. Firstly, some experiments are presented in Sub-Sect. 3.1 to analyze the behavior of the proposed approach in matching a reference pattern for different numbers of sub-arrays.

Successively, a comparative study is carried out (Sub-Sect. 3.2) by considering the available test case concerned with planar geometries and previously faced in [11].

3.1 Pattern Matching

In the first test case, the planar array consists of $N_{tot} = 4 \times N = 316$ elements equally-spaced ($d_x = d_y = \frac{\lambda}{2}$) elements arranged on a circular aperture $r = 5\lambda$ in radius. Because of the circular symmetry, the synthesis procedure is only concerned with $N = 79$ elements. Moreover, the sum pattern excitations $\underline{\zeta}$ have been fixed to those of a Taylor pattern [7] with $SLL = -35\,dB$ and $\overline{n} = 6$. On the other hand, the optimal difference $H - mode$ excitations $\underline{\varsigma}^H$ have been chosen to afford a Bayliss pattern [8] with $SLL = -40\,dB$ and $\overline{n} = 5$. The corresponding three-dimensional ($3D$) representations of the relative power distributions are reported in Fig. 2 where $u = \sin\theta\cos\phi$ and $v = \sin\theta\sin\phi$ [17], being $\theta \in [0, 90^o]$ and $\phi \in [0, 360^o]$, respectively. As regards to the compromise synthesis, the optimization has been limited to the difference $H-mode$ by exploiting the following relationship $\underline{\gamma}^E = \left\{\gamma_{rs}^E = -\gamma_{rs}^H;\ r = 1, ..., R;\ s = 1, ..., S(r)\right\}$ that holds for the $E - mode$ excitations due to the symmetry properties.

In the first experiment, the number of sub-arrays has been varied from $Q = 3$ up to $Q = 10$. Figure 3 shows the $3D$ representations of the synthesized $H - mode$ patterns. As it can be observed, the shapes of both the main lobes and the sidelobes of the compromise distributions get closer to the reference one [Fig. 2(*b*)] when the ratio $\frac{N}{Q}$ reduces. In order to better show such a trend and to efficiently represent the behavior of the side-lobes, let us analyze the *sidelobe ratio* (SLR) defined as

$$SLR\left(\phi\right) = \frac{SLL\left(\phi\right)}{max_\theta\left[AF\left(\theta, \phi\right)\right]},\ \ 0 \leq \theta < \frac{\pi}{2} \tag{11}$$

where $AF\left(\theta, \phi\right)$ indicates the array factor. By following the same guidelines in [11], the SLR has been controlled in the range $\phi \in [0^o, 80^o]$ since the $H - mode$ pattern vanishes at $\phi = 90^o$. As expected, the behavior of the SLR approximates that of the reference pattern when Q increases (Fig. 4). Such an indication is quantitatively confirmed by the statistics of the SLR values given in Tab. I as well as, pictorially, by the plots in Fig. 5 where the pattern values along the $\phi = 0^o$ cut are shown.

3.2 Comparative Assessment

To the best of the authors' knowledge, the topic of planar sub-arraying has been recently addressed only by Ares *et al.* in [11]. More in detail, a Simulated Annealing (SA) procedure has been used to determine the sub-array weights for a *pre-fixed* sub-array configuration by minimizing a suitable cost function aimed at penalizing the distance of the SLL of the compromise pattern from a prescribed value.

For comparison purposes, let us consider the same array geometry of [11]. More in detail, the elements are placed on a 20×20 regular grid ($d_x = d_y = \frac{\lambda}{2}$) lying on the xy-plane. The radius of the circular aperture of the antenna is equal to $r = 4.85\,\lambda$. The sum excitations have been fixed to those values affording a circular Taylor pattern [7] with $SLL = -35\,dB$ and $\overline{n} = 6$. Concerning the compromise solution, $Q = 3$ sub-arrays have been considered.

As far as the comparative study is concerned, the final solution of the CPM-based algorithm (i.e., definition of $\underline{c}_{opt}^{H}$ and $\underline{g}_{opt}^{H}$) has been required to present SLR values smaller than those from the SA approach [11]. Since the $PCPM$ is an excitation matching method, it has been iteratively applied by updating the reference difference pattern until the constraints on the compromise solution were satisfied. Accordingly, a succession of reference excitations $\underline{\varsigma}^{H(k)}$, $k = 1, ..., K$ have been selected. In particular, they have been fixed to those of a Bayliss difference pattern [8] with $\overline{n} = 6$ and $SLL_{ref}^{H(k)} = -25\,dB$ ($k = 1$), $SLL_{ref}^{H(k)} = -30\,dB$ ($k = 2$), and $SLL_{ref}^{H(k)} = -35\,dB$ ($k = 3$). The aggregations obtained at the end of each k-th iteration by the $PCPM$ have cost function values equal to $\Psi\left(\underline{c}_{opt}^{H(1)}\right) = 0.65 \times 10^{-1}$, $\Psi\left(\underline{c}_{opt}^{H(2)}\right) = 0.31 \times 10^{-1}$, and $\Psi\left(\underline{c}_{opt}^{H(3)}\right) = 0.27 \times 10^{-1}$, respectively. Although the application of the $PCPM$ could be further iterated by defining others reference targets, the process has been stopped at $k = k_{opt} = 3$ since the requirement [$SLR^{PCPM}(\phi) < SLR^{SA}(\phi)$, $0^o \leq \phi \leq 80^o$] has been fulfilled by the compromise solution ($\underline{c}_{opt}^{H} = \underline{c}_{opt}^{H(3)}$, $\underline{g}_{opt}^{H} = \underline{g}_{opt}^{H(3)}$). The corresponding relative power distributions are shown in Fig. 6 where the solution obtained by Ares *et. al* [11] is reported [Fig. 6(*a*)], as well. To better point out the capabilities of the iterative $PCPM$, also the plots of the SRL values (Fig. 7) and the corresponding statistics (Tab. II) are given. Moreover, in order to make the $PCPM$ results reproducible, the sub-array configurations and weights are given in Tab. III. The lists of digits of Tab. III (second row) indicate the sub-array memberships of the $N = 75$ array elements belonging to a quadrant of

the antenna aperture.

Finally, let us analyze the computational issues. The total amount of CPU-time to get the final solution was $T_{tot} = 2.6361\,[sec]$ (i.e., $T^{(1)} = 0.8148\,[sec]$, $T^{(2)} = 0.8302\,[sec]$, and $T^{(3)} = 0.9911\,[sec]$). Moreover, the number of iterations required at each step to synthesize an intermediate compromise solution is equal to $K_{opt}^{(1)} = 14$, $K_{opt}^{(2)} = 14$, and $K_{opt}^{(3)} = 17$, respectively.

4 Conclusions

In this paper, a combinatorial approach for the synthesis of sub-arrayed monopulse planar antennas has been presented. Starting from a simple and compact representation of the space of admissible solutions, the synthesis of compromise difference modes has been obtained through a path searching procedure that allows a considerable reduction of the problem complexity as well as a significant saving in terms of storage resources and CPU-time. The proposed technique has been assessed through some experiments concerned with high-dimension synthesis problems. The obtained results clearly indicate that the proposed scheme can be of interest when the number of degrees of freedom of the synthesis at hand is very large and computationally unfeasible for stochastic optimization procedures.

Acknowledgments

A. Massa wishes to thank E. Vico and C. Pedrazzani for their support. This work has been partially supported in Italy by the "*Progettazione di un Livello Fisico 'Intelligente' per Reti Mobili ad Elevata Riconfigurabilità*," Progetto di Ricerca di Interesse Nazionale - MIUR Project COFIN 2005099984.

References

[1] S. M. Sherman, *Monopulse Principles and Techniques*. Artech House, 1984.

[2] M. I. Skolnik, *Radar Handbook,* 2nd edn. McGraw-Hill, 1990.

[3] C. L. Dolph, "A current distribution for broadside arrays which optimizes the relationship between beam width and sidelobe level," *Proc. IRE*, vol. 34, no. 6, pp. 335-348, 1946.

[4] A.T. Villeneuve, "Taylor patterns for discrete arrays," *IEEE Trans. Antennas Propagat.*, vol. 32, no. 10, pp. 1089-1093, 1984.

[5] D. A. McNamara, "Direct synthesis of optimum difference patterns for discrete linear arrays using Zolotarev distribution," *IEE Proc. H Microwaves Antennas Propagat.*, vol. 140, no. 6, pp. 445-450, 1993.

[6] D.A. McNamara, "Performance of Zolotarev and modified-Zolotarev difference pattern array distributions," *IEE Proc. Microwave Antennas Propagat.*, vol. 141, no. 1, pp. 37-44, 1994.

[7] T. T. Taylor, "Design of a circular apertures for narrow beamwidth and low sidelobe," *Trans. IRE Antennas Propagat.*, vol. 8, pp. 17-22, 1960.

[8] E. T. Bayliss, "Design of monopulse antenna difference patterns with low sidelobes," *Bell System Tech. Journal*, vol. 47, pp. 623-640, 1968.

[9] A. K. Singh, P. Kumar, T. Chakravarty, G. Singh, and S. Bhooshan, "A novel digital beamformer with low angle resolution for vehicle tracking radar," Progress in Electromagnetics Research, PIER, vol. 66, pp. 229-237, 2006.

[10] D. A. McNamara, "Synthesis of sub-arrayed monopulse linear arrays through matching of independently optimum sum and difference excitations," *IEE Proc. H Microwaves Antennas Propagat.*, vol. 135, no. 5, pp. 293-296, 1988.

[11] F. Ares, S. R. Rengarajan, J. A. Rodriguez, and E. Moreno, "Optimal compromise among sum and difference patterns through sub-arraying," *Proc. IEEE Antennas Propagat. Symp.*, Baltimore, MD, USA, Jul. 1996, pp. 1142-1145.

[12] P. Lopez, J. A. Rodriguez, F. Ares, E. and Moreno, "Subarray weighting for difference patterns of monopulse antennas: joint optimization of subarray configurations and weights," *IEEE Trans. Antennas Propagat.*, vol. 49, no. 11, pp. 1606-1608, 2001.

[13] S. Caorsi, A. Massa, M. Pastorino, and A. Randazzo, "Optimization of the difference patterns for monopulse antennas by a hybrid real/integer-coded differential evolution method," *IEEE Trans. Antennas Propagat.*, vol. 53, no. 1, pp. 372-376, 2005.

[14] M. D'Urso, T. Isernia, and E. F. Meliado', E. F., "An effective hybrid approach for the optimal synthesis of monopulse antennas," *IEEE Trans. Antennas Propagat.*, vol. 55, no. 4, pp. 1059-1066, 2007.

[15] L. Manica, P. Rocca, A. Martini, and A. Massa, A., "An innovative approach based on a tree-searching algorithm for the optimal matching of independently optimum sum and difference excitations," *IEEE Trans. Antennas Propagat.*, 2007. (in press)

[16] W. D. Fisher, "On grouping for maximum homogeneity," *American Statistical Journal*, 789-798, 1958.

[17] R. S. Elliott, *Antenna Theory and Design.* Wiley-Interscience IEEE Press, 2003.

FIGURE CAPTIONS

- **Figure 1.** *DAG* Representation.

- **Figure 2.** *Pattern Matching* ($N = 316$, $d = \frac{\lambda}{2}$, $r = 5\lambda$) - Relative power distribution of the reference (*a*) Taylor sum pattern ($SLL = -35\,dB$, $\overline{n} = 6$) [7] and of the (*b*) $H-mode$ Bayliss difference pattern ($SLL = -40\,dB$, $\overline{n} = 5$) [8], respectively.

- **Figure 3.** *Pattern Matching* ($N = 316$, $d = \frac{\lambda}{2}$, $r = 5\lambda$) - Relative power distribution of the synthesized $H - mode$ difference pattern when (*a*) $Q = 3$, (*b*) $Q = 4$, (*c*) $Q = 6$, and (*d*) $Q = 10$.

- **Figure 4.** *Pattern Matching* ($N = 316$, $d = \frac{\lambda}{2}$, $r = 5\lambda$) - Plots of the SLR values of the Bayliss pattern ($SLL = -40\,dB$, $\overline{n} = 5$) [8] and of the compromise $H-mode$ difference patterns when $Q = 3,\ 4,\ 6,\ 10$ ($\phi \in [-80^o,\ 80^o]$).

- **Figure 5.** *Pattern Matching* ($N = 316$, $d = \frac{\lambda}{2}$, $r = 5\lambda$) - Azimuthal ($\phi = 0^o$) plots of the relative power of the Bayliss pattern ($SLL = -40\,dB$, $\overline{n} = 5$) [8] and of the compromise $H - mode$ patterns when $Q = 3,\ 4,\ 6,\ 10$.

- **Figure 6.** *Comparative Assessment* ($N = 300$, $d = \frac{\lambda}{2}$, $r = 4.85\lambda$, $Q = 3$) - Relative power distribution of the $H - mode$ compromise pattern synthesized with (*a*) the SA approach [11] and the $PCPM$ when the Reference Bayliss pattern $\overline{n} = 6$ [8] presents a sidelobe level equal to (*b*) $SLL_{ref}^{H(1)} = -25\,dB$, (*c*) $SLL_{ref}^{H(2)} = -30\,dB$, and (*d*) $SLL_{ref}^{H(3)} = -35\,dB$.

- **Figure 7.** *Comparative Assessment* ($N = 300$, $d = \frac{\lambda}{2}$, $r = 4.85\lambda$, $Q = 3$) - Plots of the SLR values of the compromise $H - mode$ difference patterns synthesized by the SA approach [11] and the $PCPM$ when the Reference Bayliss pattern $\overline{n} = 6$ [8] presents a sidelobe level equal to $SLL_{ref}^{H(1)} = -25\,dB$, $SLL_{ref}^{H(2)} = -30\,dB$, and (*d*) $SLL_{ref}^{H(3)} = -35\,dB$ ($\phi \in [-80^o,\ 80^o]$).

TABLE CAPTIONS

- **Table I.** *Pattern Matching* ($N = 316$, $d = \frac{\lambda}{2}$, $r = 5\lambda$) - Statistics of the SLR values in Fig. 3.

- **Table II.** *Comparative Assessment* ($N = 300$, $d = \frac{\lambda}{2}$, $r = 4.85\lambda$, $Q = 3$) - Statistics of the SLR values of the $H - mode$ difference pattern synthesized with the SA approach [11] and with the iterative $PCPM$ (Reference Bayliss pattern $\overline{n} = 6$ [8]: $SLL_{ref}^{H(1)} = -25\,dB$, $SLL_{ref}^{H(2)} = -30\,dB$, and $SLL_{ref}^{H(3)} = -35\,dB$).

- **Table III.** *Comparative Assessment* ($N = 300$, $d = \frac{\lambda}{2}$, $r = 4.85\lambda$, $Q = 3$) - Sub-array configurations and weights obtained with the $PCPM$ (Reference Bayliss pattern $\overline{n} = 6$ [8]: $SLL_{ref}^{H(1)} = -25\,dB$, $SLL_{ref}^{H(2)} = -30\,dB$, and $SLL_{ref}^{H(3)} = -35\,dB$).

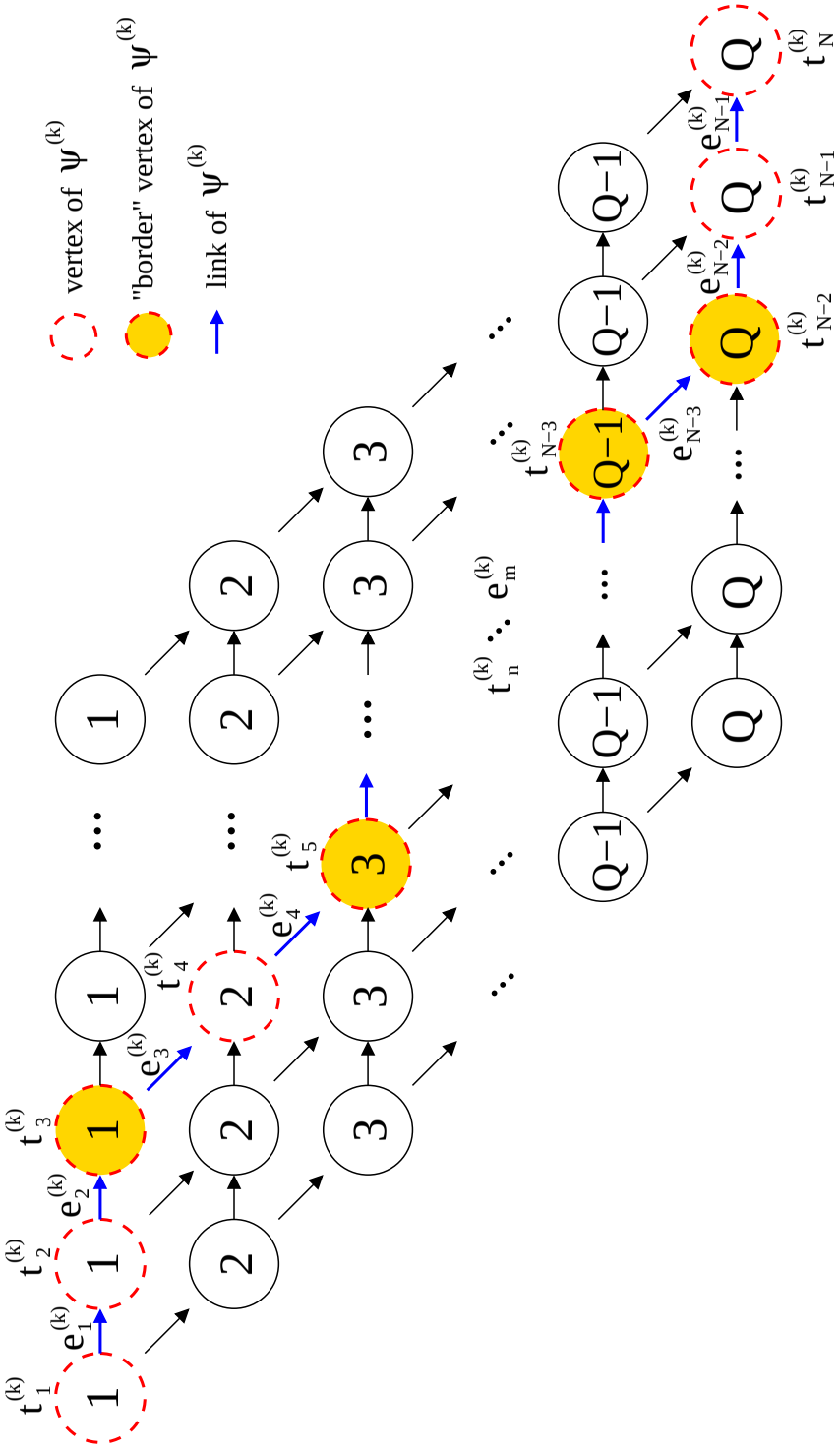

Fig. 1 - P. Rocca *et al.*, “An effective excitation matching method ...”

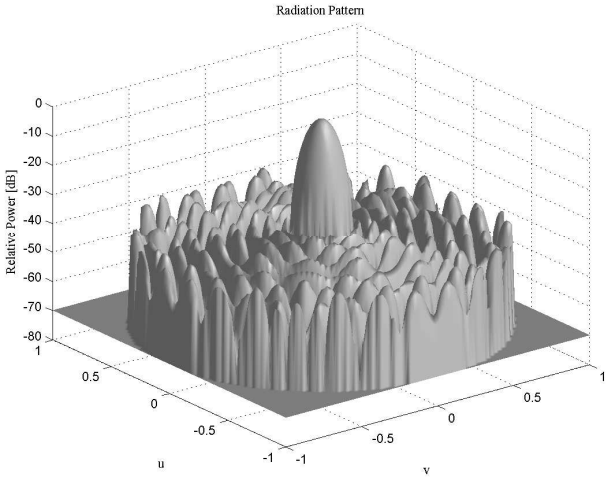

(a)

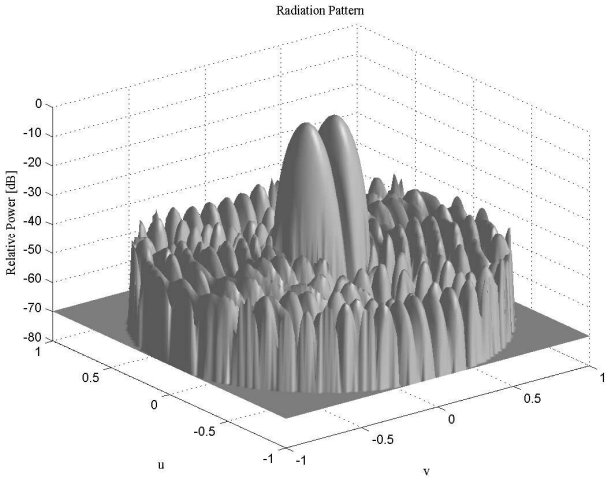

(b)

Fig. 2 - P. Rocca *et al.*, "An effective excitation matching method ..."

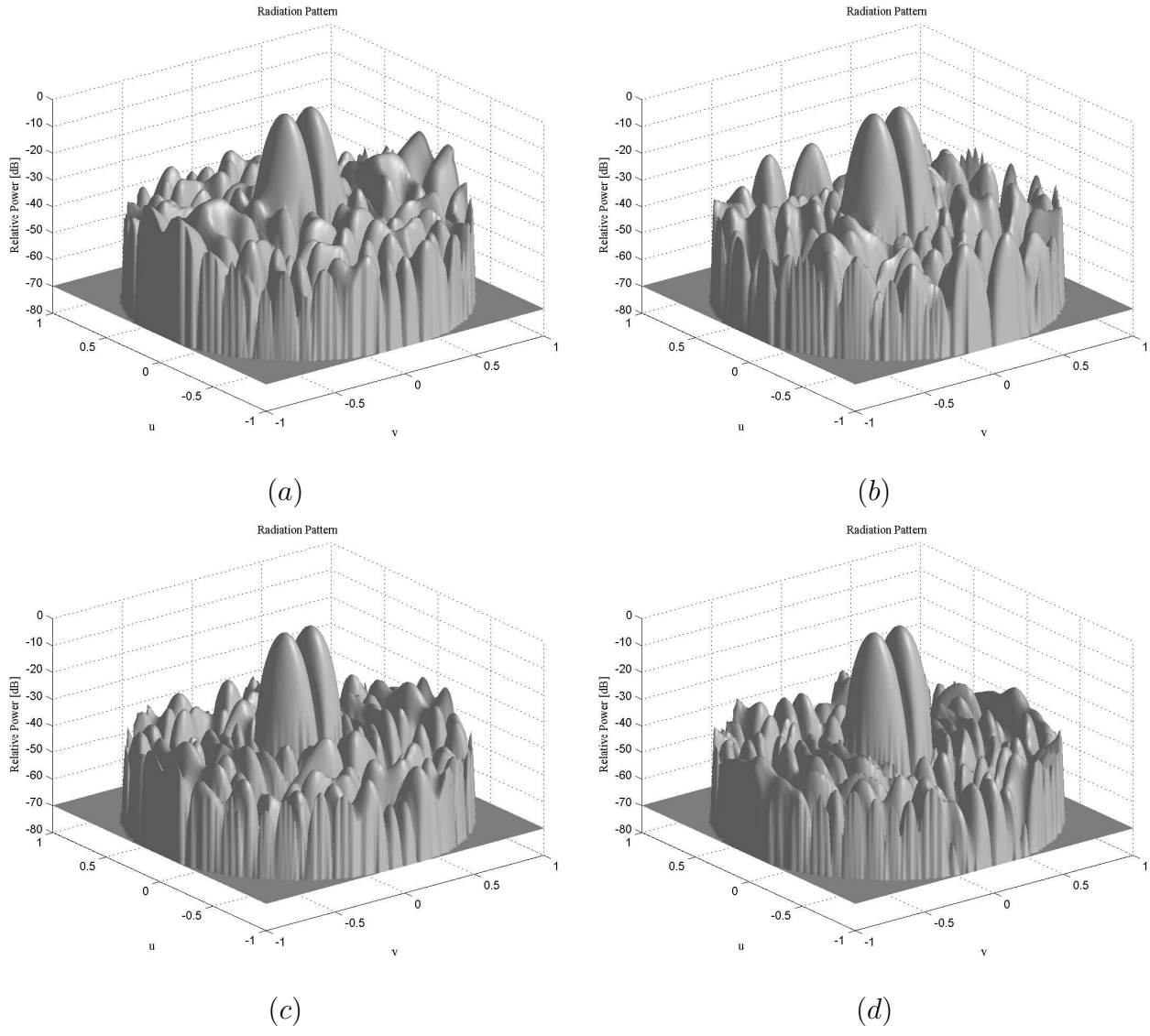

Fig. 3 - P. Rocca *et al.*, “An effective excitation matching method ...”

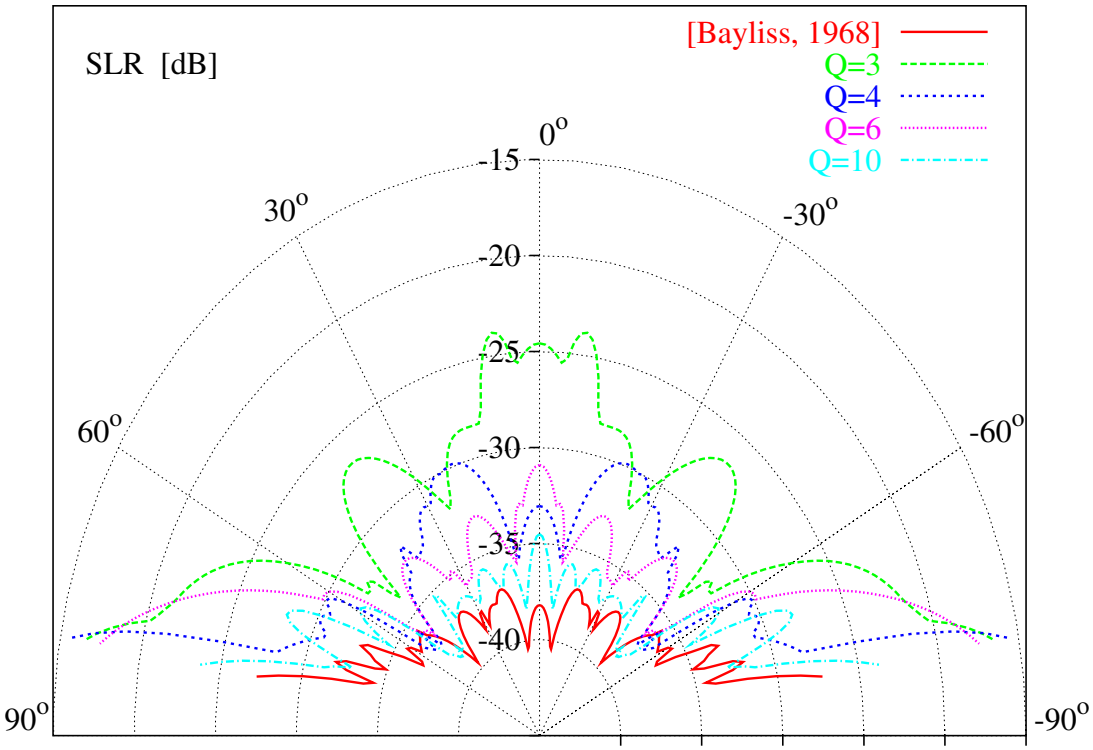

Fig. 4 - P. Rocca *et al.,* "An effective excitation matching method ..."

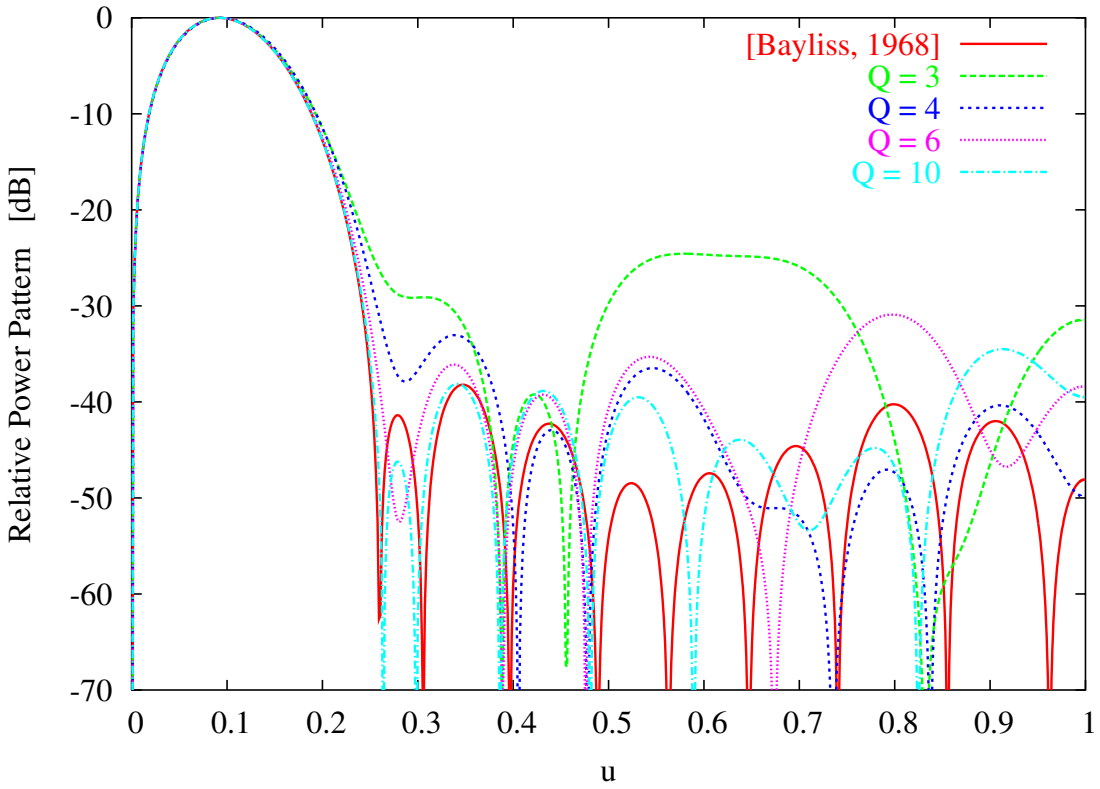

Fig. 5 - P. Rocca *et al.*, "An effective excitation matching method ..."

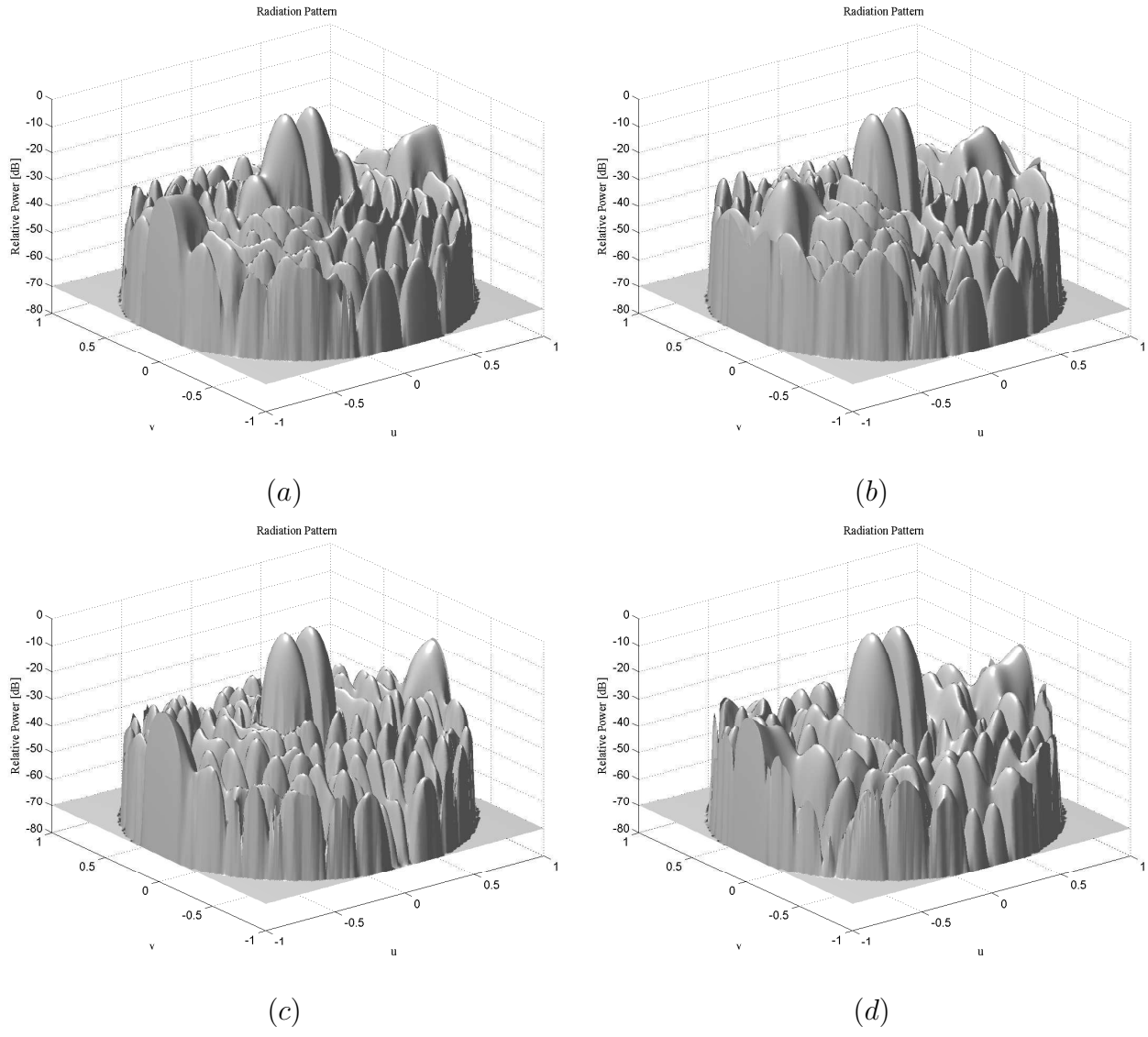

Fig. 6 - P. Rocca *et al.*, “An effective excitation matching method ...”

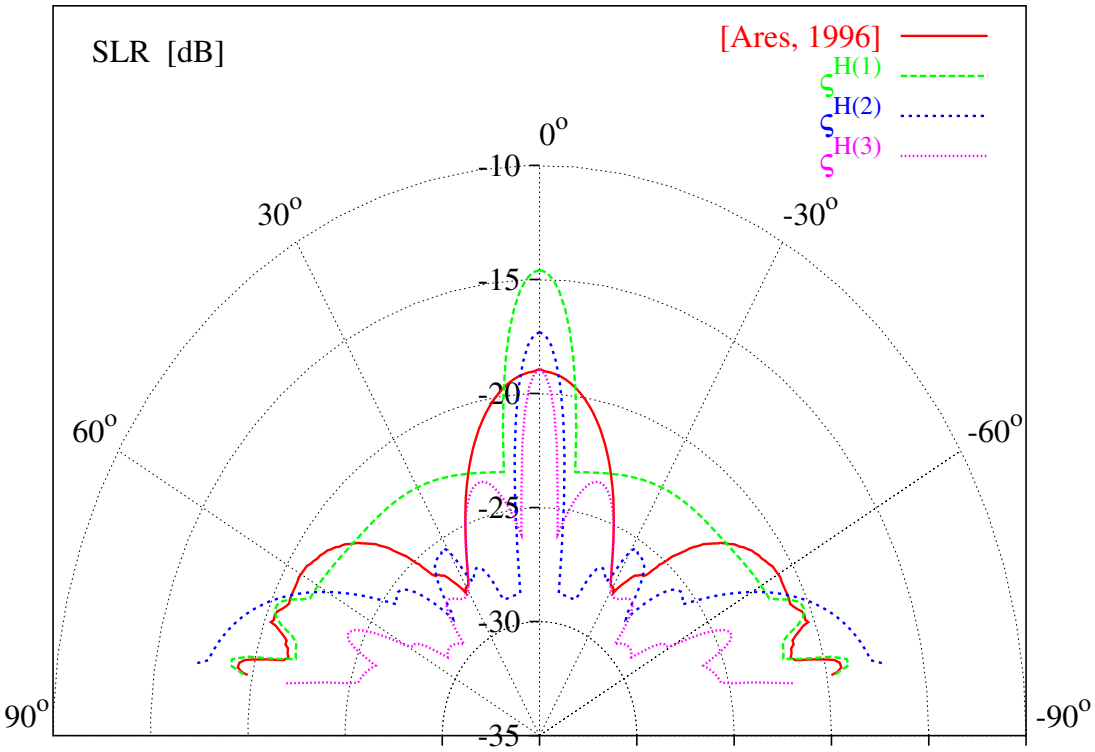

Fig. 7 - P. Rocca *et al.*, "An effective excitation matching method ..."

$[dB]$	$min\{SLR\}$	$max\{SLR\}$	$av\{SLR\}$	$var\{SLR\}$
$Reference$ [8]	-40.44	-27.29	-36.68	6.05
$Q = 3$	-33.82	-16.48	-26.74	14.26
$Q = 4$	-37.32	-15.68	-31.56	15.11
$Q = 6$	-36.67	-17.47	-31.25	26.30
$Q = 10$	-38.72	-23.75	-34.77	11.46

$[dB]$	$min\{SLR\}$	$max\{SLR\}$	$av\{SLR\}$	$var\{SLR\}$
SA [11]	-27.70	-18.93	-22.52	6.41
$CPM:\ SLL_{ref}^{H(1)} = -25\,dB$	-23.30	-14.58	-21.48	3.93
$CPM:\ SLL_{ref}^{H(2)} = -30\,dB$	-28.78	-16.95	-24.08	14.15
$CPM:\ SLL_{ref}^{H(3)} = -35\,dB$	-29.43	-18.94	-25.87	5.74

	$SLL_{ref}^{H(1)} = -25\,dB$	$SLL_{ref}^{H(2)} = -30\,dB$	$SLL_{ref}^{H(k_{opt})} = -35\,dB$
$\underline{c}$	1 1 1 1 1 2 2 1 1 1 2 2 2 1 1 1 2 2 2 3 1 1 1 2 2 2 3 3 1 1 1 2 2 2 3 3 3 1 1 1 2 2 2 3 3 3 1 1 1 2 2 2 3 3 3 1 1 1 2 2 3 3 3 3 3 1 1 1 2 2 3 3 3 3 3	1 1 1 1 1 1 2 1 1 1 2 2 2 1 1 2 2 2 2 2 1 1 2 2 2 3 3 3 1 1 2 2 3 3 3 3 3 1 1 2 2 3 3 3 3 3 1 1 2 2 3 3 3 3 3 1 1 2 2 3 3 3 3 3 3 1 1 2 2 3 3 3 3 3 3	1 1 1 1 1 1 1 1 1 1 1 1 2 1 1 1 2 2 2 2 1 1 2 2 2 2 2 2 1 1 2 2 3 3 3 2 2 1 1 2 2 3 3 3 3 2 1 1 2 2 3 3 3 3 3 1 1 2 3 3 3 3 3 3 2 1 1 2 3 3 3 3 3 3 2
g_1	0.4668	0.3337	0.3355
g_2	1.3435	0.9763	0.9381
g_3	2.1736	1.6091	1.4469

Tab. III - P. Rocca *et al.,* "An effective excitation matching method ..."